



THE UNIVERSITY *of* EDINBURGH

## Edinburgh Research Explorer

### Actin dynamics regulation by TTC7A/PI4KIII $\alpha$ limits DNA damage and cell death under confinement

**Citation for published version:**

Gajardo, T, Bernard, M, Lô, M, Turck, E, Leveau, C, El-Daher, MT, Deslys, A, Panikulam, P, Menche, C, Kurowska, M, Le Lay, G, Barbier, L, Moshous, D, Neven, B, Farin, HF, Fischer, A, Ménasché, G, de Saint Basile, G, Vargas, P & Sepulveda, FE 2023, 'Actin dynamics regulation by TTC7A/PI4KIII $\alpha$  limits DNA damage and cell death under confinement', *Journal of Allergy and Clinical Immunology*, vol. 152, no. 4, pp. 949-960. <https://doi.org/10.1016/j.jaci.2023.06.016>

**Digital Object Identifier (DOI):**

[10.1016/j.jaci.2023.06.016](https://doi.org/10.1016/j.jaci.2023.06.016)

**Link:**

[Link to publication record in Edinburgh Research Explorer](#)

**Document Version:**

Publisher's PDF, also known as Version of record

**Published In:**

Journal of Allergy and Clinical Immunology

**General rights**

Copyright for the publications made accessible via the Edinburgh Research Explorer is retained by the author(s) and / or other copyright owners and it is a condition of accessing these publications that users recognise and abide by the legal requirements associated with these rights.

**Take down policy**

The University of Edinburgh has made every reasonable effort to ensure that Edinburgh Research Explorer content complies with UK legislation. If you believe that the public display of this file breaches copyright please contact [openaccess@ed.ac.uk](mailto:openaccess@ed.ac.uk) providing details, and we will remove access to the work immediately and investigate your claim.

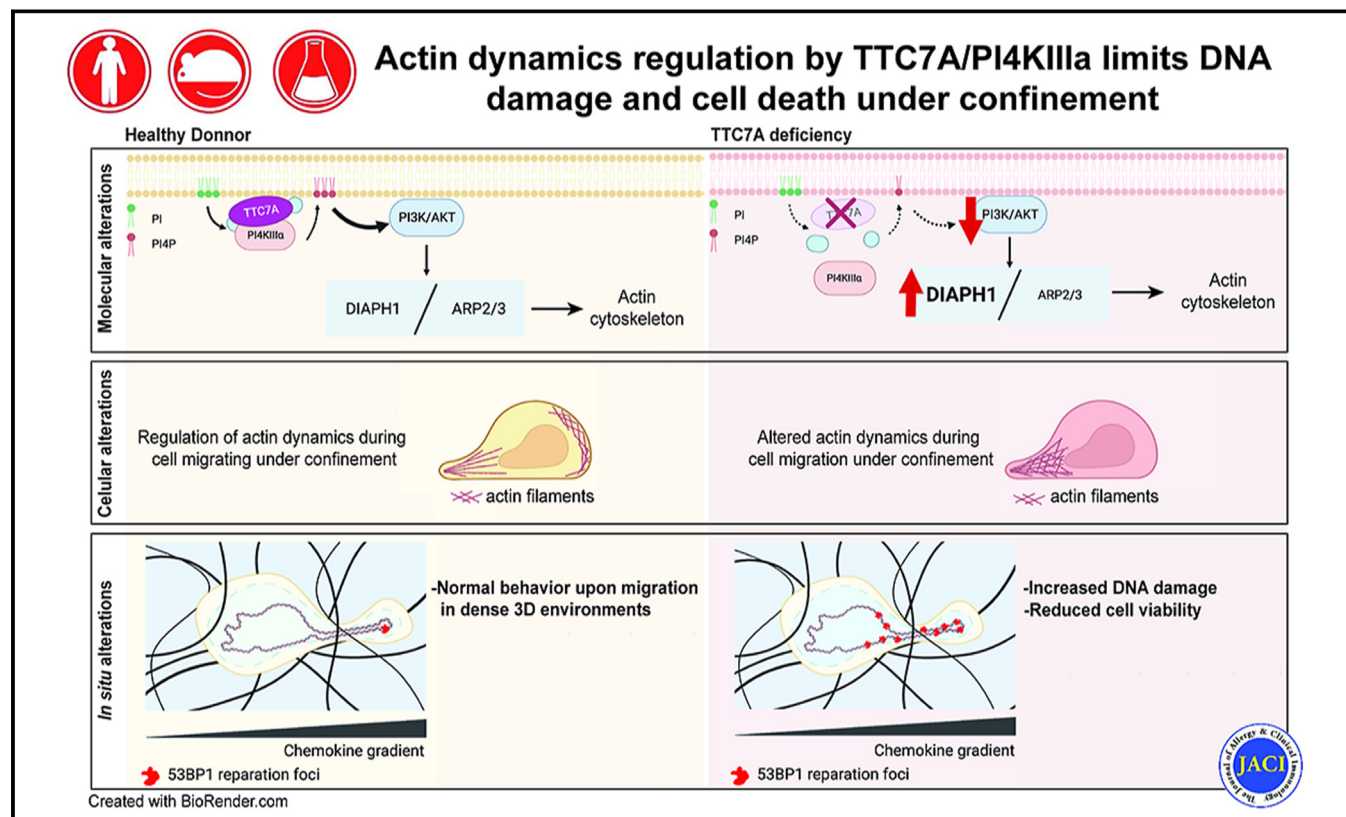


# Actin dynamics regulation by TTC7A/PI4KIII $\alpha$ limits DNA damage and cell death under confinement



Tania Gajardo, PhD,<sup>a,b</sup> Mathilde Bernard, MS,<sup>c,d\*</sup> Marie Lô, MS,<sup>a,b\*</sup> Elisa Turck, MS,<sup>a,b</sup> Claire Leveau, PhD,<sup>a,b</sup> Marie-Thérèse El-Daher, PhD,<sup>a,b</sup> Alexandre Deslys, MS,<sup>e</sup> Patricia Panikulam, MS,<sup>a,b</sup> Constantin Menche, MS,<sup>f,g</sup> Mathieu Kurowska, MS,<sup>a,b</sup> Gregoire Le Lay, MS,<sup>c,d</sup> Lucie Barbier, PhD,<sup>c,d</sup> Despina Moshous, MD, PhD,<sup>b,h</sup> Bénédicte Neven, MD, PhD,<sup>b,h</sup> Henner F. Farin, PhD,<sup>f,g</sup> Alain Fischer, MD, PhD,<sup>b,h,i</sup> Gaël Ménasché, PhD,<sup>a,b</sup> Geneviève de Saint Basile, MD, PhD,<sup>a,b,j</sup> Pablo Vargas, PhD,<sup>c,d,e</sup> and Fernando E. Sepulveda, PhD<sup>a,b,k</sup> *Paris, France; and Frankfurt am Main, Germany*

## GRAPHICAL ABSTRACT



From <sup>a</sup>the Molecular Basis of Altered Immune Homeostasis Laboratory, Institut National de la Santé et de la Recherche Médicale (INSERM) Unite Mixte de Recherche (UMR) 1163; <sup>b</sup>the Imagine Institute, Université de Paris Cité; <sup>c</sup>the UMR 144, Institut Curie; <sup>d</sup>the Institut Pierre-Gilles de Gennes, Paris Sciences and Letters Research University; <sup>e</sup>Leukomotion Lab, Université de Paris Cité, CNRS, INSERM, Institut Necker-Enfants Malades, F-75015 Paris; <sup>f</sup>the Pediatric Immunology Hematology and Rheumatology Department, and <sup>g</sup>the Centre d'Etude des Déficits Immunitaires, Necker-Enfants Malades University Hospital, Assistance Publique-Hôpitaux de Paris, Université Paris Cité; <sup>h</sup>the Collège de France; and <sup>i</sup>the CNRS, Paris; <sup>j</sup>the Georg-Speyer-Haus, Institute for Tumor Biology and Experimental Therapy; and <sup>k</sup>the Frankfurt Cancer Institute, Goethe University Frankfurt.

\*These authors contributed equally to this work.

Received for publication September 6, 2022; revised May 24, 2023; accepted for publication June 1, 2023.

Available online June 29, 2023.

Corresponding authors: Fernando E. Sepulveda, PhD, INSERM U1163, Imagine Institute, 24 Boulevard de Montparnasse, F-75015 Paris, France. E-mail: [fernando.sepulveda@inserm.fr](mailto:fernando.sepulveda@inserm.fr). Or: Pablo Vargas, PhD, Group leader Leukomotion Lab, INSERM U1151, 160 Rue de Vaugirard, F-75015, Paris, France. E-mail: [pablo.vargas@inserm.fr](mailto:pablo.vargas@inserm.fr) and [pablo.vargas@curie.fr](mailto:pablo.vargas@curie.fr).

The CrossMark symbol notifies online readers when updates have been made to the article such as errata or minor corrections

0091-6749

© 2023 The Authors. Published by Elsevier Inc. on behalf of the American Academy of Allergy, Asthma & Immunology. This is an open access article under the CC BY license (<http://creativecommons.org/licenses/by/4.0/>).

<https://doi.org/10.1016/j.jaci.2023.06.016>

**Background:** The actin cytoskeleton has a crucial role in the maintenance of the immune homeostasis by controlling various cellular processes, including cell migration. Mutations in *TTC7A* have been described as the cause of a primary immunodeficiency associated to different degrees of gut involvement and alterations in the actin cytoskeleton dynamics. **Objectives:** This study investigates the impact of *TTC7A* deficiency in immune homeostasis. In particular, the role of the *TTC7A*/phosphatidylinositol 4 kinase type III  $\alpha$  pathway in the control of leukocyte migration and actin dynamics. **Methods:** Microfabricated devices were leveraged to study cell migration and actin dynamics of murine and patient-derived leukocytes under confinement at the single-cell level. **Results:** We show that *TTC7A*-deficient lymphocytes exhibit an altered cell migration and reduced capacity to deform through narrow gaps. Mechanistically, *TTC7A*-deficient phenotype resulted from impaired phosphoinositide signaling, leading to the downregulation of the phosphoinositide 3-kinase/AKT/RHOA regulatory axis and imbalanced actin cytoskeleton dynamics. *TTC7A*-associated phenotype resulted in impaired cell motility, accumulation of DNA damage, and increased cell death in dense 3-dimensional gels in the presence of chemokines. **Conclusions:** These results highlight a novel role of *TTC7A* as a critical regulator of lymphocyte migration. Impairment of this cellular function is likely to contribute to the pathophysiology underlying progressive immunodeficiency in patients. (*J Allergy Clin Immunol* 2023;152:949-60.)

**Key words:** *TTC7A*, cell migration, actin dynamics, nuclear deformation, cell survival under confinement

Autosomal recessive biallelic mutations in *TTC7A* have been identified as the cause of an immune and gastrointestinal disorder of variable severity.<sup>1-4</sup> Depending on the type of mutation, gastrointestinal symptoms can present as very early-onset inflammatory bowel disease or multiple intestinal atresia. On the other hand, immune manifestations of patients who are *TTC7A*-deficient range from mild lymphopenia to combined immunodeficiency.<sup>5</sup> In general, patients who are *TTC7A*-deficient develop a progressive lymphopenia, leading to increased susceptibility to infections.

*TTC7A* contains 9 tetratricopeptide repeat domains, which have been proposed to act as scaffold for protein complexes.<sup>6</sup> Our group and others have described diverse functions mediated by *TTC7A*. *In vitro*, cells from patients who are *TTC7A*-deficient present with disrupted actin cytoskeleton and cell polarity through the increase of RHOA-mediated signaling.<sup>1</sup> *TTC7A* also interacts with the supramolecular complex containing phosphatidylinositol 4 kinase type III  $\alpha$  (PI4KIII $\alpha$ ), EFR3B, and HYCC1 (also known as FAM126A), in the plasma membrane.<sup>7</sup> PI4KIII $\alpha$  is required for the synthesis of phosphatidylinositol 4-phosphate (PI4P), which is necessary for plasma membrane identity, cell survival, and cell polarity.<sup>8,9</sup> *TTC7A* can also be localized in the nucleus, participating in the regulation of chromatin structure and nuclear organization.<sup>10</sup> Finally, in mice, *Ttc7* controls hematopoietic stem cells' stemness.<sup>11</sup> Despite our improved understanding of the different cellular functions of *TTC7A*, the pathophysiological mechanisms underlying *TTC7A*-associated immunodeficiency are not fully characterized.

In the present study, we leverage microfabricated devices to investigate the impact of *TTC7A* deficiency on leukocyte

#### Abbreviations used

3D:	3-dimensional
ARP2/3:	Actin-related protein 2/3 complex
B-LCL:	Lymphoblastoid B-cell lines
ctrl:	Control
DC:	Dendritic cell
fsn:	Flaky skin
HD:	Healthy donor
iDC:	Immature dendritic cell
mDC:	LPS-activated dendritic cell
mDia1:	Diaphanous-related formin 1
pAKT:	Phosphorylation levels of AKT
PI3K:	Phosphoinositide 3-kinase
PI4KIII $\alpha$ :	Phosphatidylinositol 4 kinase type III $\alpha$
PI4P:	Phosphatidylinositol 4-phosphate

migratory capacity at the single-cell level. We found that *TTC7A*-deficient lymphocytes presented an increased cell speed compared to control cells, but a reduced cellular (and nuclear) deformation capacity when migrating along micrometric spaces. Mechanistically, *TTC7A* deficiency disrupted actin cytoskeleton polymerization downstream of the PI4KIII $\alpha$ /phosphoinositide 3-kinase (PI3K)/AKT signaling pathway. Notably, confinement of lymphocytes from patients who are *TTC7A*-deficient in dense CCL21-containing 3-dimensional (3D) microenvironments resulted in increased DNA damage and cell death. We propose that altered actin dynamics observed in *TTC7A*-deficient lymphocytes modifies their migratory capacity and survival in complex 3D microenvironments, possibly contributing to progressive lymphopenia observed in patients who are *TTC7A*-deficient.

## METHODS

Additional methods are available in this article's Online Repository (available at [www.jacionline.org](http://www.jacionline.org)).

### Patients

Our patients who are *TTC7A*-deficient have been previously reported<sup>2,4</sup> and gave their consent to participate in the study. Patients with the following biallelic mutations in *TTC7A* were included: L304fsX59, E71K, R325Q. A density gradient using lymphocyte separation media (Eurobio, France) was performed to recover the PBMCs from patients and healthy donors (HDs). Cells were activated either with 5  $\mu$ g/mL PHA (Sigma-Aldrich, St Louis, Mo) and 100 U/mL of IL-2 (PeproTech, Thermo Fisher Scientific, Waltham, Mass) for 3 days and cultured in RPMI-1640 medium supplemented with 10% FBS and 1% penicillin/streptomycin (Gibco, Thermo Fisher Scientific), or with Transact (Miltenyi Biotec, Gaithersburg, Md) following instructions from the manufacturer. To obtain monocytes, CD14 cells were purified using CD14<sup>+</sup> selection kit (BD Biosciences, San Jose, Calif). Lymphoblastoid B-cell lines (B-LCLs) and stably transduced cell lines were generated as previously described.<sup>2,10</sup>

### Microdevices

Microdevices were prepared as previously described.<sup>12</sup> Briefly, devices were fabricated using polydimethylsiloxane and custom-

made molds, coated with 10  $\mu\text{g}/\text{mL}$  fibronectin from bovine plasma (Sigma-Aldrich, St Louis, Mo) for 1 hour. Migration was recorded using a Zeiss Axio Observer Z1 (Hamamatsu digital camera C11440; Carl Zeiss, Oberkochen, Germany) microscope, with a time lapse of 1 or 2 minutes using a 10 $\times$  (numerical aperture 0.45) dry objective. The image analysis was done using ImageJ (National Institutes of Health, Bethesda, Md). Briefly, kymographs for each channel were generated using a semiautomatic macro, and single-cell trajectories were manually isolated. Trajectories were then analyzed with a custom-made MATLAB (MathWorks, Natick, Mass) code to determine the cell speed. For the analysis of constrictions, the same macro was used as the generation of the kymographs and then manual quantification was performed to obtain the percentage of cells that pass. We assessed the following outcomes: (1) pass, (2) not-pass and turn, and (3) not-pass and blocked. Turn cells were considered as those that reach the constriction and turn back in  $\leq 10$  timeframes. Blocked cells correspond to cells that reached the constriction and stopped without passing or turning back for  $> 10$  timeframes. Chemotaxis in constricted environments was achieved by loading in a secondary well a solution containing 200 ng/mL of CXCL12 (Pepro-Tech, Thermo Fisher Scientific, Waltham, Mass) 30 minutes before acquisition.

### Statistics

All data analysis was performed with GraphPad Prism 9 for MacOS (GraphPad Software, Boston, Mass). Statistical differences were considered when  $P < .05$ ,  $P < .01$ ,  $P < .001$ , and  $P < .0001$ .

Data obtained from migration experiments were evaluated for normal distribution using the D'Agostino-Pearson test, and comparisons between conditions were performed using Mann-Whitney/unpaired  $t$ -test (for 2 conditions) or 2-way ANOVA test (for  $> 2$  conditions), depending on the normality result. The passage through microconstrictions follows a binomial distribution and  $P$  values were calculated using the chi-square method for each experiment and pair of samples compared.

## RESULTS

### Ttc7 regulates 1D migration of immature murine dendritic cells

Gut organoids derived from patients who are TTC7A-deficient present with an altered actin cytoskeleton polarity due to increased RHOA signaling.<sup>1,2</sup> This pathway also controls leukocyte migration under confinement.<sup>13,14</sup> Hence, we thought to determine the impact of Ttc7 deficiency on leukocyte migration. In a first step, we generated bone marrow-derived DCs from flaky skin (fsn) mice (natural mutant deficient for *Ttc7*). We observed that Ttc7 was not required for DC differentiation, nor for Toll-like receptor response *in vitro* (Fig E1, A and B in this article's Online Repository at [www.jacionline.org](http://www.jacionline.org)). To assess whether Ttc7 was required for DC motility, we compared the migration of immature DCs (iDCs) and LPS-activated DCs (mDCs) from control and fsn mice using microchannels, in which cells migrate along micrometric tubes.<sup>14</sup> As expected, control DCs increased speed on LPS treatment (Fig 1, A and B).<sup>15</sup> Interestingly, Ttc7-deficient immature DCs (iDC<sup>fsn</sup>) were as fast as mature DCs from both control (ctrl) and fsn mice (mDC<sup>ctrl</sup> and mDC<sup>fsn</sup>, respectively) at different levels of confinement (ie, 4- and

8- $\mu\text{m}$ -wide microchannels) (Fig 1, A and B and Fig E1, C). Similar results were obtained when comparing speed of control and Ttc7-deficient T cells (Fig E1, D). Therefore, we hypothesized that Ttc7 is a critical regulator of leukocytes migration under confinement.

Because DC migration in microchannels strongly relies on actin,<sup>15,16</sup> we sought to determine the impact of Ttc7 deficiency in actin polymerization. We had shown that in iDC<sup>ctrl</sup> slow and fast motility phases in microchannels are regulated by the nucleation activities of actin-related protein 2/3 complex (Arp2/3) (at the cell front) and diaphanous-related formin 1 (mDia1) (at the cell rear), whereas fast motility of mDCs mostly depends on mDia1 function.<sup>15,16</sup> Accordingly, iDC<sup>ctrl</sup> presented with a bimodal concentration of F-actin at the cell front and rear, while mDC<sup>ctrl</sup> presented F-actin structures preferentially at the back of the cell (ie, reduced front/back ratio of actin staining) (Fig 1, C and D and Fig E1, E and F). Notably, both iDC<sup>fsn</sup> and mDC<sup>fsn</sup> accumulated F-actin and mDia1 preferentially at the cell rear (Fig 1, C and D and Fig E1, E and F). Of note, Arp2 distribution was not affected by Ttc7 deficiency (Fig 1, C and D and Fig E1, E and F).

To determine whether increased speed of iDC<sup>fsn</sup> was caused by an elevated Rhoa/Rock-mediated signaling,<sup>2</sup> we inhibited Rock activity (ie, Y-27632 treatment) and its downstream target Myosin II (ie, blebbistatin treatment) in control and Ttc7-deficient DCs. Both treatments decreased speed in iDC<sup>ctrl</sup> and iDC<sup>fsn</sup> (Fig E1, G and H). We further assessed the contribution of mDia1 to iDC<sup>fsn</sup> phenotype.<sup>17</sup> To do so, we used the formins inhibitor Smifh2, which reduced the speed of iDC<sup>fsn</sup> while not affecting iDC<sup>ctrl</sup> (Fig 1, E). Moreover, Smifh2 treatment of iDC<sup>fsn</sup> led to F-actin redistribution from rear to the front of the cell (Fig 1, F and G). Collectively, these data support that Ttc7 deficiency in iDC<sup>fsn</sup> promotes mDia1-dependent actin nucleation at the cell rear, increasing cell speed in microchannels.

### TTC7A controls human T-cell migration

To determine the impact of TTC7A deficiency on migration of human lymphocytes, we assessed spontaneous speed of blood T cells derived from HDs and different patients carrying biallelic mutations in TTC7A, migrating in 1D-confined microchannels. We assessed the impact of 3 different TTC7A deleterious mutations (TTC7A<sup>L304fsX59</sup>, TTC7A<sup>E71K</sup>, and TTC7A<sup>R325Q</sup>).<sup>2,4</sup> Human activated T cells had persistent trajectories (Fig 2, A and Video E1 in this article's Online Repository at [www.jacionline.org](http://www.jacionline.org)). T cells derived from patients who are TTC7A-deficient were faster than their control counterparts (Fig 2, A and B and Video E1). Consistent with a general role of TTC7A in the control of leukocyte migration, similar observations were made with patient-derived B-LCLs and primary monocytes (Fig 2, C and Fig E2, A-C and Video E2 in this article's Online Repository at [www.jacionline.org](http://www.jacionline.org)). In all these cases (and thus independent of the underlying mutation), TTC7A-deficient cells were faster than control cells. Increased speed of TTC7A-deficient cells was independent of the coating, as patient-derived T-cell blasts were faster than controls in fibronectin (Fig 2, B) and collagen coated-channels (Fig E2, D). Notably, transduction of patient-derived B-LCLs with wild type TTC7A (but not with TTC7A<sup>E71K</sup>), restored normal cell speed (Fig E2, D).

Human T-cell blasts rely on ROCK and MYOSIN II activities for actin polymerization and contractile force generation during migration in microchannels (Fig 2, E and F). HD T-cell blasts had



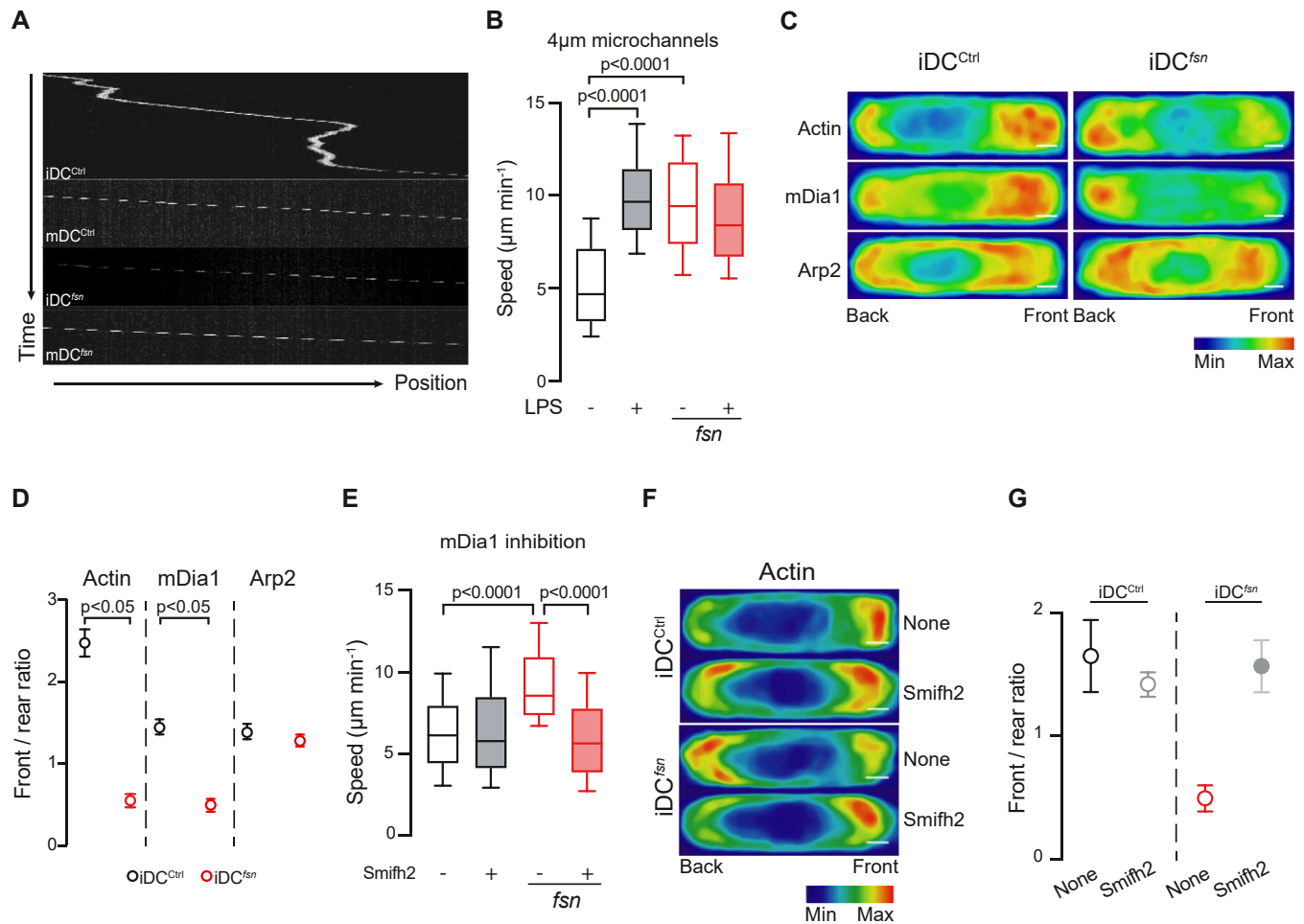


**FIG 1.** Ttc7 controls 1D migration of murine DCs by regulating actin polymerization. DC<sup>ctrl</sup> and DC<sup>fsn</sup> migrating in 4  $\mu\text{m}$   $\times$  5  $\mu\text{m}$  fibronectin-coated microchannels. **(A)** Representative kymographs of iDC<sup>ctrl</sup>, mDC<sup>ctrl</sup>, iDC<sup>fsn</sup>, and mDC<sup>fsn</sup> migrating in microchannels. **(B)** Mean instantaneous speed of iDC<sup>ctrl</sup> (black empty bars), mDC<sup>ctrl</sup> (black filled bars), iDC<sup>fsn</sup> (red empty bars), and mDC<sup>fsn</sup> (red filled bars) ( $n = 6$ ,  $n \geq 200$  cells/condition). Boxes include 80% of the points; bars represent the higher and lower 10% of points. **(C)** Density maps of iDC<sup>ctrl</sup> and iDC<sup>fsn</sup> stained with actin-phalloidin ( $n > 100$  cells/condition), mDia1 ( $n > 55$  cells/condition), and Arp2 ( $n > 55$  cells/condition). Bar = 2  $\mu\text{m}$ . **(D)** Front/rear ratio of the signal intensity shown in C for iDC<sup>ctrl</sup> (black empty circles) and iDC<sup>fsn</sup> (red empty circles). Actin-phalloidin ( $n = 4$ ), mDia1 ( $n = 3$ ), and Arp2 ( $n = 2$ ). **(E)** iDC<sup>ctrl</sup> (black bars) and iDC<sup>fsn</sup> (red bars) were treated (filled bars) or not (empty bars) with Smifh2 ( $n = 3$ ,  $n \geq 100$  cells/condition). **(F)** Actin-phalloidin density maps of iDC<sup>ctrl</sup> (top panels) and iDC<sup>fsn</sup> (bottom panels) treated or not with Smifh2 ( $n \geq 60$  cells/condition). Bar = 2  $\mu\text{m}$ . **(G)** Front/rear ratio of the signal intensity shown in F for iDC<sup>ctrl</sup> (black empty circles), Smifh2-treated iDC<sup>ctrl</sup> (gray empty circles), iDC<sup>fsn</sup> (red empty circles), and Smifh2-treated iDC<sup>fsn</sup> (gray-filled circles) ( $n = 2$ ). Two-way ANOVA or Mann-Whitney tests were used to evaluate statistical significance. Max, Maximum; Min, minimum.

a bimodal distribution of actin in the front and rear of the cell during migration in microchannels (Fig 2, G and H). In agreement with their increased speed, TTC7A-deficient T-cell blasts exhibited an increased F-actin polymerization at the cell rear (Fig 2, G and H). To evaluate the contribution of DIAPH1 (human homolog of mDia1) and ARP2/3 to this phenotype, we treated HD and TTC7A-deficient T-cell blasts with Smifh2 and CK-666 and measured cell migration. Our data showed that DIAPH1 (but not ARP2/3) inhibition restored cell speed of TTC7A-deficient cells to control values (Fig 2, I and Fig E2, E). These results suggest that increased migration speed under confinement of TTC7A-deficient T-cell blasts, involve an aberrant activation of DIAPH1 and increased F-actin polymerization at the cell rear, highlighting TTC7A as a critical regulator of actin polymerization during human T-cell migration.

### Increased cell speed observed in TTC7A-deficient cells is mediated by reduced PI4KIII $\alpha$ activity

TTC7A plays a critical role in the assembly and function of the multiprotein complex involving PI4KIII $\alpha$ , EFR3A, and HYCC1.<sup>18</sup> TTC7A deficiency leads to an impaired formation and localization of this complex, hindering PI4KIII $\alpha$  activity and the subsequent phosphoinositide metabolism<sup>3,6</sup> (Fig 3, A). To characterize the contribution of PI4KIII $\alpha$  in lymphocyte migration under confinement, we treated control human T-cell blasts with 2 different chemical inhibitors of PI4KIII $\alpha$ , BF-738735 and GSK-A1. In both cases, we observed that PI4KIII $\alpha$  inhibition increased cell speed (Fig 3, B), suggesting that the enhanced motility of patient-derived cells could be caused by a defective PI4KIII $\alpha$  activity. To address this question, we supplemented control and TTC7A-deficient T-cell blasts with

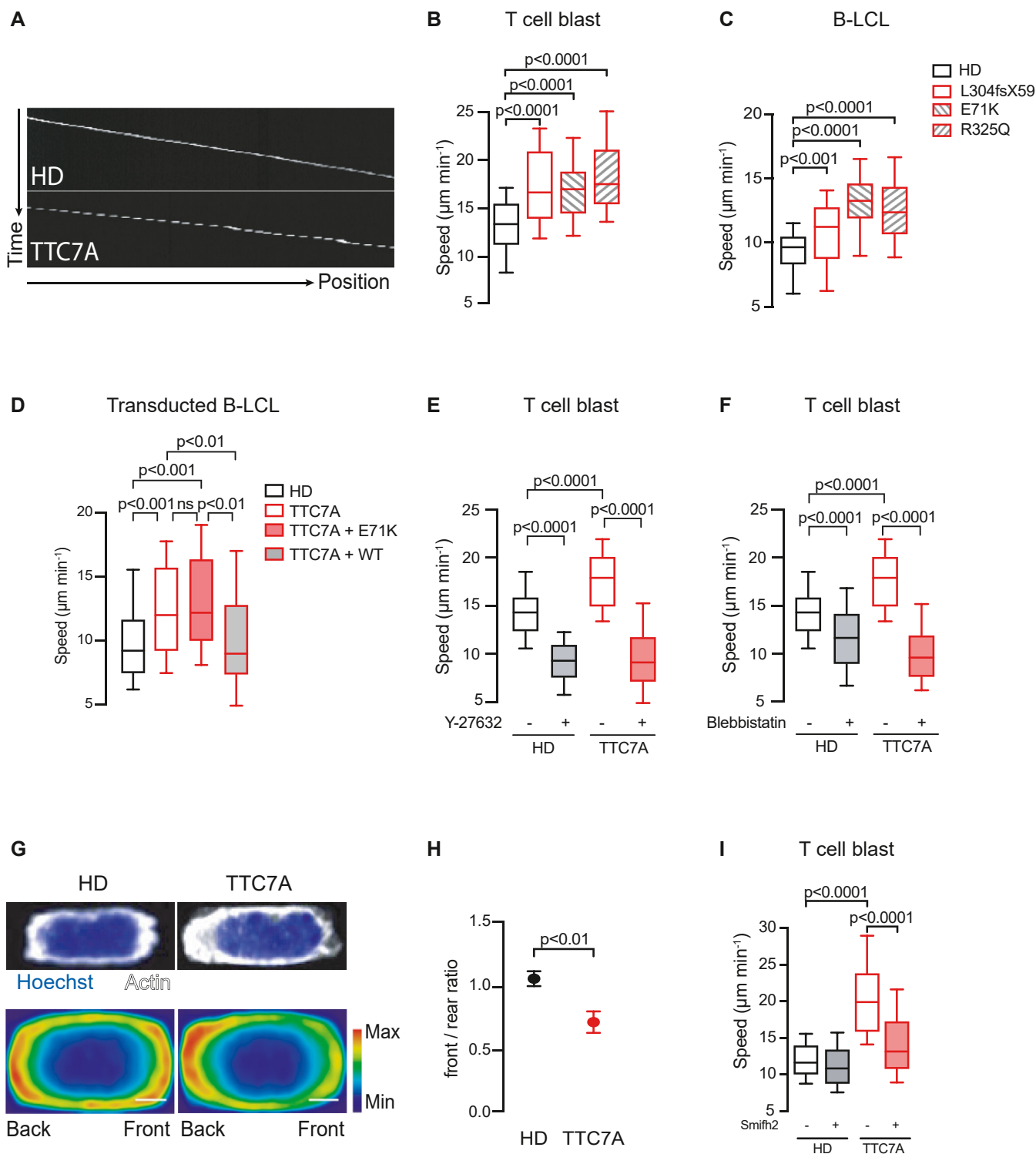


**FIG. 2.** TTC7A controls migration of human T cells. Human HD and TTC7A cells migrating in  $4 \mu\text{m} \times 5 \mu\text{m}$  microchannels. **(A)** Representative kymographs from HD and TTC7A T cells. **(B)** Mean instantaneous speed of HD and TTC7A. TTC7A<sup>L304fsX59</sup> (1 patient,  $n = 1$ ), TTC7A<sup>E71K</sup> (5 patients,  $n = 11$ ), and TTC7A<sup>R325Q</sup> (1 patient,  $n = 3$ ) ( $n = 7$ ,  $n > 90$  cells/condition). **(C)** Mean instantaneous speed of HD and TTC7A-deficient B-LCL in  $8 \mu\text{m} \times 5 \mu\text{m}$  microchannels. TTC7A<sup>L304fsX59</sup> (1 patient,  $n = 3$ ), TTC7A<sup>E71K</sup> (3 patients,  $n = 8$ ), and TTC7A<sup>R325Q</sup> (1 patient,  $n = 3$ ) ( $n > 90$  cells/condition). **(D)** HD (black empty bar), TTC7A-deficient (red empty bar), TTC7A-deficient transduced with mutated TTC7A<sup>E71K</sup> (red filled bar), and TTC7A-deficient transduced with TTC7A<sup>WT</sup> (gray filled bar) B-LCLs migrating in  $8 \mu\text{m} \times 5 \mu\text{m}$  microchannels ( $n = 2$ ,  $n > 70$  cells/condition). **(E,F)** HD (black bars) and TTC7A-deficient (red bars) cells treated (filled bars) or not (empty bars) with **(E)** Y-27632 ( $n = 2$ ,  $n \geq 200$  cells/condition) or **(F)** with blebbistatin ( $n = 2$ ,  $n \geq 150$  cells/condition). **(G)** Representative Hoechst (blue) and actin-phalloidin (white) immunofluorescence (top panels) from HD and TTC7A T cells. Actin-phalloidin density maps (bottom panels) ( $n > 120$  cells/condition). Bar =  $2 \mu\text{m}$ . **(H)** Front/rear ratio of the signal intensity shown in **F** ( $n = 3$ ). **(I)** Mean instantaneous speed of HD (black bars) and TTC7A (red bars) cells treated (filled bars) or not (empty bars) with Smifh2 ( $n = 3$ ,  $n > 80$  cells/condition). Two-way ANOVA or Mann-Whitney tests were used to evaluate statistical significance.

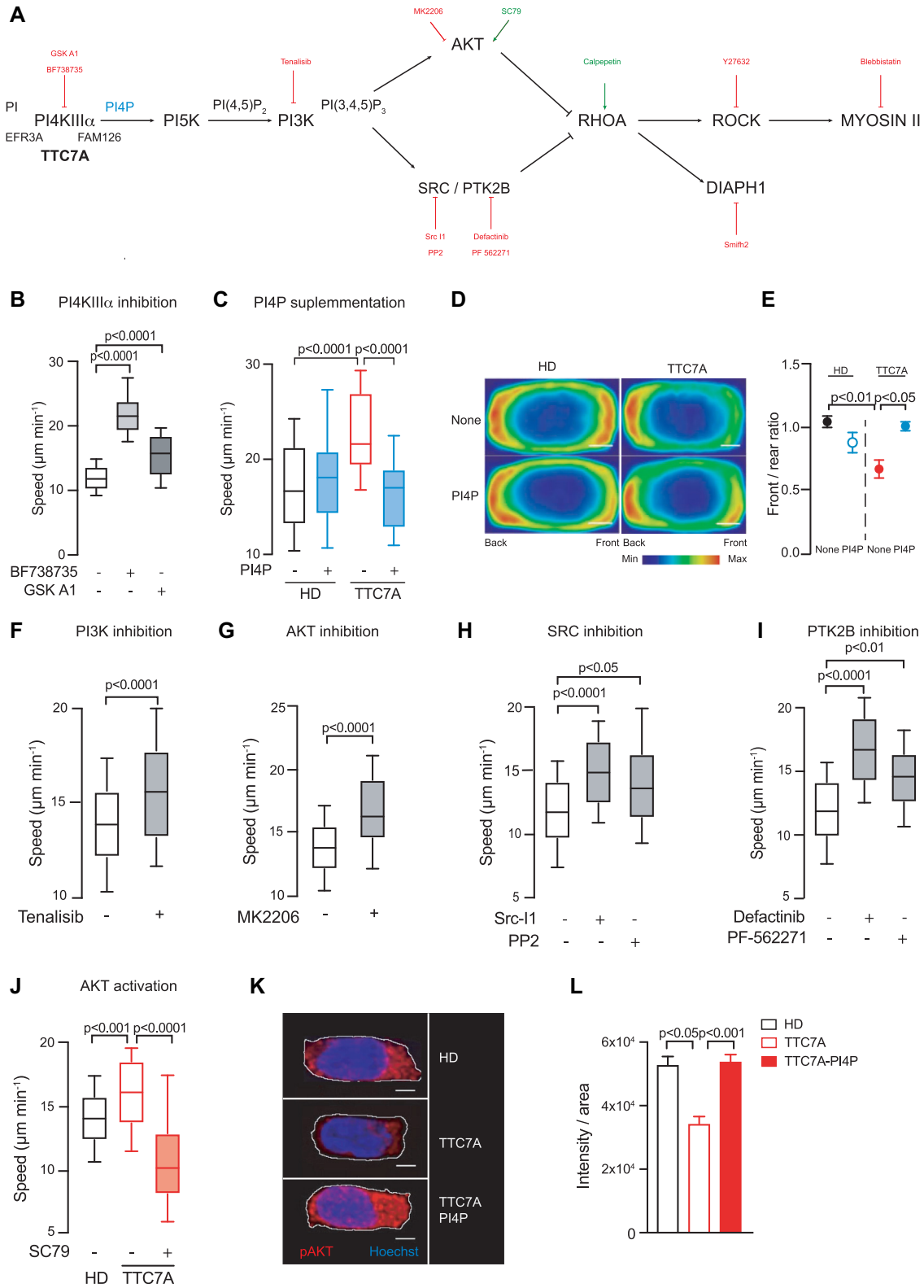


**FIG 3.** Kinase activity of PI4KIII $\alpha$  controls leukocyte migration. **(A)** Schematic representation of the PI4KIII $\alpha$ /TTC7A signaling pathway, including the drugs used. Inhibitors (red), activators (green), and PI4P (blue). **(B–J)** Mean instantaneous speed of HD (black bars) and/or TTC7A-deficient (red bars) T cells treated (filled bars) or not (empty bars) with different drugs. Migration was assessed in 4  $\mu$ m  $\times$  5  $\mu$ m microchannels (n = 3). **(B)** HD cells treated with BF-738735 and GSK-A1 (n  $\geq$  160 cells/condition). **(C)** HD and TTC7A cells supplemented (blue filled bars) or not with PI4P (n  $\geq$  100 cells/condition). **(D)** Actin-phalloidin density maps of **(C)**. Bar = 2  $\mu$ m. **(E)** Front/rear ratio of the signal intensity shown in **(D)** (n = 3, n > 130 cells/

exogenous PI4P (the metabolite produced by PI4KIII $\alpha$ ) or with PI(3,4,5)P<sub>3</sub> (a downstream phospholipid of the pathway) and assessed 1D-confined cell migration. PI4P and PI(3,4,5)P<sub>3</sub> supplementation did not affect migration of control cells (Fig 3, C and Fig E3, A in this article's Online Repository at [www.jacionline.org](http://www.jacionline.org)). In contrast, both phospholipids reduced migration speed of TTC7A-deficient T-cell blasts and redistributed the F-actin pool toward the front of the cell (Fig 3, C-E and Fig E3, A). On the other hand, treatment of TTC7A-deficient cells with irrelevant phospholipids such as PI3P and phosphatidylcholine did not affect cell speed (Fig E3, B). PI4P availability is crucial for the phosphoinositide cascade, PI3K activity, and further downstream signaling.<sup>19</sup> Moreover, PI3K/AKT pathway modulates RHOA/ROCK activity and thus actin dynamics (Fig 3, A).<sup>20</sup> We therefore investigated the contribution of PI3K and downstream signaling (ie, AKT, SRC, and PTK2B) in T-cell migration under confinement. The treatment of control T-cell blasts with specific chemical inhibitor for PI3K increased cell speed, recapitulating the phenotype observed in TTC7A-deficient cells (Fig 3, F). Similarly, AKT, SRC, and PTK2B inhibition in control cells also increased cell speed (Fig 3, G-I). In agreement with the hypothesis of reduced PI4KIII $\alpha$ /PI3K signaling as the cause of altered actin dynamics in TTC7A-deficient cells, exogenous activation of AKT by SC79 in TTC7A-deficient T-cell blasts restored cell speed (Fig 3, J). To further characterize the impact of TTC7A-deficiency in AKT activity, we compared the phosphorylation levels of AKT (pAKT) in HD and TTC7A-deficient cells while migrating under confinement. Even if total levels of AKT were similar, we observed lower pAKT in TTC7A-deficient T-cell blasts compared to control, and PI4P supplementation increased pAKT levels of TTC7A-deficient cells (Fig 3, K and L and Fig E3, C). These results demonstrate that TTC7A deficiency disrupts the activity of the PI4KIII $\alpha$ /PI3K/AKT/SRC axis and alters human T-cell motility, highlighting the critical regulatory role of this pathway in actin polymerization during lymphocyte migration under confinement.

### Impairment of PI4KIII $\alpha$ /DIAPH1/actin function in TTC7A-deficient cells disrupts the capacity to migrate through micrometric pores and irregularly confined microenvironments

*In vivo*, leukocyte migration occurs in complex microenvironments requiring a high degree of cell deformability.<sup>21</sup> To characterize the impact of TTC7A deficiency in the capacity of lymphocytes to deform their nucleus, we studied the behavior of control and TTC7A-deficient T-cell blasts while migrating through 8- $\mu$ m microchannels carrying constrictions of 1.5- or 2.0- $\mu$ m width and 15- $\mu$ m length (Fig 4, A). In agreement with previous experiments, cells spontaneously migrated in 8- $\mu$ m channels devoid of constrictions, and TTC7A-deficient T-cell

blasts were faster than control cells (Fig E4, A in this article's Online Repository at [www.jacionline.org](http://www.jacionline.org)). When facing 1.5- $\mu$ m constrictions, TTC7A deficiency strongly reduced the capacity of T-cell blasts and B-LCLs to spontaneously pass through a 1.5- $\mu$ m constriction (Fig 4, B and Fig E4, B). Moreover, TTC7A-deficient cells that still passed the constriction took longer than control cells did (Fig 4, C and Fig E4, C). Similar results were observed in Ttc7-deficient mouse T cells (Fig E4, D). Notably, transduction of TTC7A-deficient B-LCLs with wild-type TTC7A (but not TTC7A<sup>E71K</sup>), restored normal cell passage (Fig E4, B and C). Of note, when cells were forced to pass the constriction (on CXCL12 stimulation) (Fig E4, E), TTC7A-deficient T-cell blasts passed at a similar level as control counterparts did, but passage time was still increased (Fig E4, F and G).

Cell passage through constrictions requires a high degree of cellular (and nuclear) deformation. In murine DCs, it has been shown that this process rely on an ARP2/3-dependent perinuclear actin polymerization.<sup>22</sup> Accordingly, ARP2/3 inhibition reduced T-cell passage in both control and TTC7A-deficient conditions (Fig E4, H). Next, we aimed to determine whether the reduced capacity of TTC7A-deficient cells to pass the constrictions was related to a defective nuclear deformation. Thus, we assessed nuclear deformation in the fraction of cells that failed to pass the constriction. We defined 4 different situations depending on the capacity of the nucleus to enter the constriction: First, cells that did not deform their nucleus at all (group I), cells in which the nucleus entered <33% of the constriction (group II), between 33% and 66% of the constriction (group III), and 100% of the constriction (group IV) (Fig 4, D). Blocked control T cells had an equal repartition among the 4 different groups (Fig 4, E and F), suggesting that cell blockage was not determined by impaired capacity to deform the nucleus. In contrast, a large majority of TTC7A-deficient T-cell blasts failed to enter their nucleus in the constriction (group I) (Fig 4, E and F), suggesting that the reduced capacity of TTC7A-deficient cells to pass through micrometric spaces was caused by an impaired capacity to deform their nucleus.

To determine whether the reduced passage rate of TTC7A-deficient cells in 1.5- $\mu$ m constrictions was caused by alterations in the PI4KIII $\alpha$  signaling pathway, we supplemented TTC7A-deficient cells with PI4P or PI(3,4,5)P<sub>3</sub>. We observed that phospholipid treatment restored the capacity of TTC7A-deficient cells to migrate through 1.5- $\mu$ m constrictions and reduced the time required to do so (Fig 4, B and C and Fig E4, I). DIAPH1 inhibition by Smifh2 treatment also restored the capacity of TTC7A-deficient cells to pass through 1.5- $\mu$ m constrictions (Fig 4, B). In both cases (PI4P and Smifh2 treatments), restoration of cell passage correlated with reestablishment of the nuclear deformability of nonpassing TTC7A-deficient T-cell blasts to a level comparable with that of control cells (Fig 4, F). These data suggest that the altered actin polymerization characterizing

condition). (F) HD cells treated with tenalisib ( $n \geq 160$  cells/condition). (G) HD cells treated with MK2206-2HCl ( $n \geq 180$  cells/condition). (H) HD cell treated with SRC-inhibitors ( $n \geq 130$  cells/condition). (I) HD cells treated with PTK2B inhibitors ( $n \geq 150$  cells/condition). (J) TTC7A cells treated with SC79 ( $n \geq 100$  cells/condition). (K) Immunofluorescence of cells stained with pAKT (red) and Hoechst (blue). HD (top panel), TTC7A (middle panel), TTC7A-PI4P (bottom panel). Bar = 2  $\mu$ m. (L) Quantification of intensity/area of K for HD (black bars) and PI4P-treated (red filled bars) or not (red empty bars) TTC7A-deficient T cells ( $n = 3$ ,  $n > 95$  cells/condition). Fluorescence intensity determined using Icy software (Institut Pasteur, Paris, France). Two-way ANOVA or Mann-Whitney tests were used to evaluate statistical significance.



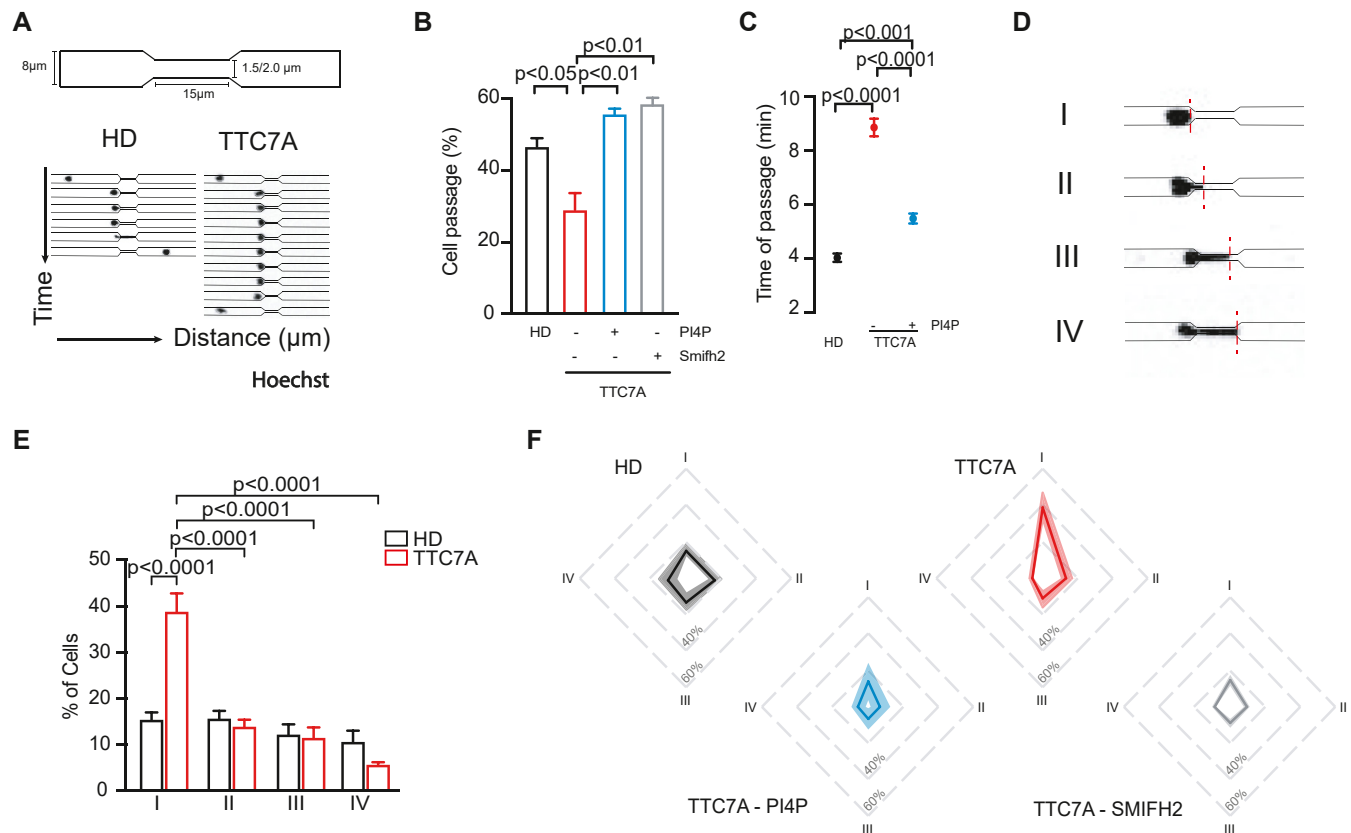


**FIG 4.** TTC7A is necessary for T-cell blast to pass through constrictions. **(A)** Schematic representation of the migration assay through constricted microchannels. Lower panel depicts HD (left panel) and TTC7A-deficient (right panel) T-cell blasts passing through a 1.5- $\mu$ m-wide, 15- $\mu$ m-long constriction. **(B)** Percentage of HD (black empty bar) and TTC7A (red empty bar) T-cell blasts passing through 1.5- $\mu$ m constrictions. TTC7A cells supplemented with PI4P (blue empty bar) or with Smifh2 (gray empty bar) ( $n = 4$ ,  $n \geq 270$  cells/condition). The proportion of passing cells follows a binomial distribution, hence  $P$  values were calculated with the chi-square method. **(C)** Average time of passage for HD (black circles) and TTC7A T-cell blasts treated (blue circles) or not (red circles) with PI4P ( $n = 3$ ). **(D)** Classification of the nucleus deformation in nonpassing cells. I: no deformation; II: deformation until 33% of the constriction; III: deformation between 33% and 66% of the constriction; IV: deformation covering all (100%) of the constriction. **(E)** Distribution of nuclear deformation of nonpassing HD (black empty bars) and TTC7A (red empty bars) T cells. **(F)** Distribution of nuclear deformation of nonpassing cells for HD (black), TTC7A (red), TTC7A-PI4P (blue), and TTC7A-Smifh2 (gray) T cells. Line depicts the mean value and the shadow the standard deviation ( $n = 4$ ). Two-way ANOVA was used for statistical analysis in **C** and **E**.

TTC7A-deficient cells impaired the capacity to pass through micrometric pores.

To evaluate the impact of TTC7A deficiency in leukocyte migration in a more complex microenvironment in which cells undergo frequent nuclear deformations during their migration (Fig E5, A in this article's Online Repository at [www.jacionline.org](http://www.jacionline.org)), we assessed cell motility in dense collagen gels. Analysis of random migration showed that TTC7A-deficient T-cell blasts were similar to control cells in their capacity to explore their microenvironment despite a slightly reduced mean speed (Fig 5, A and B). Of note, TTC7A deficiency did not affect the chemotactic response to CCL21, as both responded to the chemokine (Fig 5, C). To determine the contribution of PI4KIII $\alpha$  signaling pathway in collagen migration, we assessed T-cell migration on inhibition of PI4KIII $\alpha$ . GSK-A1 treatment reduced speed in a dose-dependent manner in both control and TTC7A-deficient T-cell blasts, highlighting the critical role of PI4KIII $\alpha$  signaling to T-cell migration. Consistent with an impaired PI4KIII $\alpha$

signaling in TTC7A-deficient cells, the latter were more sensitive to GSK-A1 treatment, because the same concentration of the drug reduced the speed of TTC7A-deficient cells more than it did in control cells (Fig 5, D). Similarly, exploratory capacity, quantified by the mean-squared displacement, of TTC7A-deficient cells was more affected than that of GSK-A1-treated control cells (Fig 5, E and F). These results show that TTC7A/PI4KIII $\alpha$  signaling pathway is required for T-cell migration in complex 3D microenvironments.

### TTC7A is essential for preservation of genome integrity and cell survival when migrating in complex 3D microenvironments

Cell migration in irregular microenvironments has been associated to transient nuclear envelope ruptures and DNA damage.<sup>22,23</sup> Therefore, we hypothesized that the alterations in nuclear deformation capacity observed in TTC7A-deficient

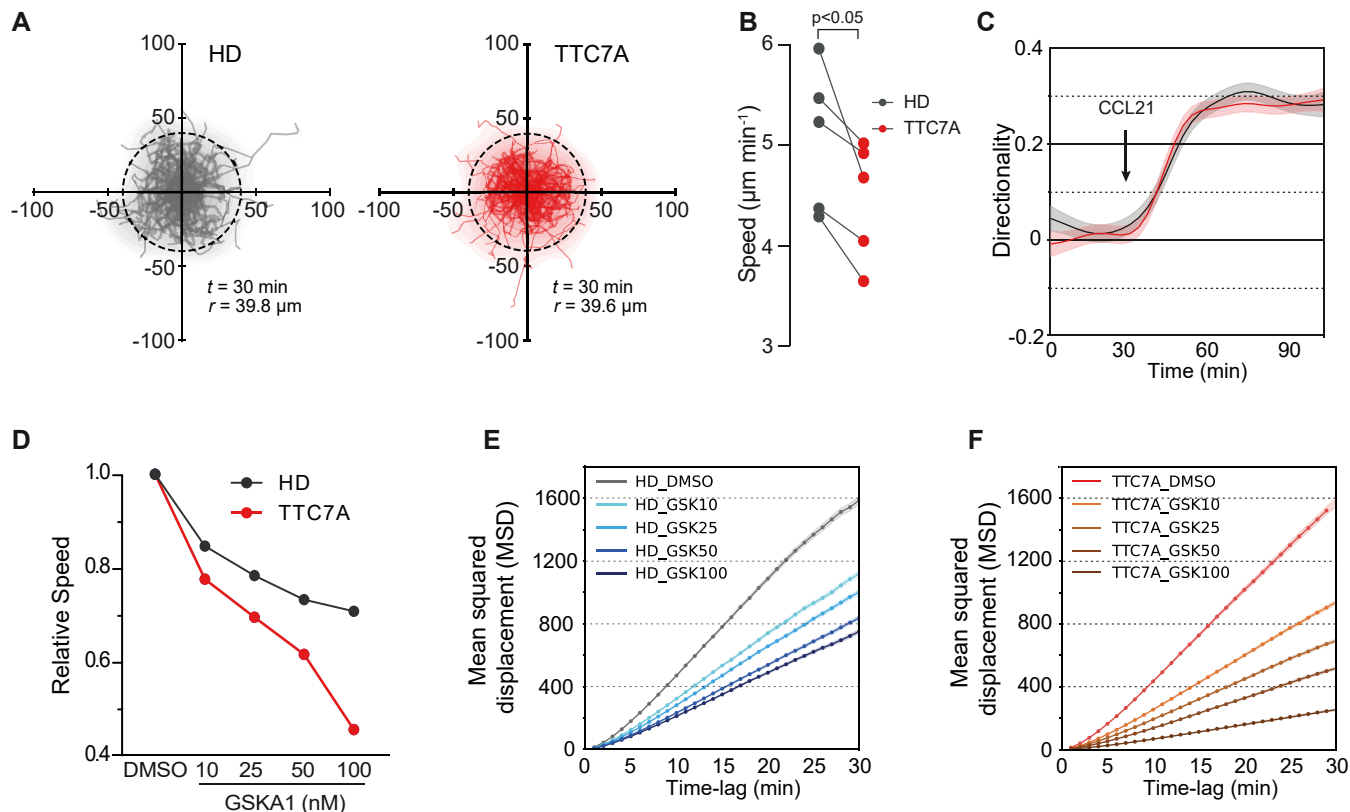


**FIG 5.** TTC7A is needed to optimize leukocyte motility in dense 3D collagen gels. **(A)** Representative trajectories of HD (gray) and TTC7A (red) T-cell blasts migrating in 2 mg/mL collagen gel. Fifty trajectories of 30-minute duration were randomly sampled and plotted. The radius  $r$  of the plotted circle corresponds to the root mean-squared displacement computed for all trajectories and for the given time-lag  $t = 30$  minutes. **(B)** Average speed of >500 single-cell trajectories per experiment ( $n = 6$ ). **(C)** Directionality over time in response to CCL21 added at 30 minutes after random migration. **(D-F)** GSK-A1 dose-dependent response: HD and TTC7A-deficient T-cell blasts were treated with different doses of PI4KIII $\alpha$  inhibitor. The dimethyl sulfoxide (DMSO) maximum volume concentration (1/12,000) was used as control. For both samples, relative speed corresponds to the average cell speed of each treatment divided by the average speed of DMSO-treated cells **(D)**. For each condition, the mean-squared displacement was computed for all trajectories **(E-F)**. All graphs are a representative result of at least 2 independent experiments.

lymphocytes may negatively impact genomic stability and survival when migrating in complex 3D microenvironments. We assessed the viability of control and TTC7A-deficient T-cell blasts, either seeded in dense collagen gels for 48 hours or in suspension (Fig 6, A). While cell viability was comparable between control and TTC7A-deficient cells in both settings (Fig 6, B and C), the addition of the chemokine CCL21 to collagen gels significantly increased cell mortality of TTC7A-deficient T-cell blasts compared to controls (Fig 6, B and C). Of note, CCL21-induced mortality of TTC7A-deficient cells was not observed in suspension (Fig E6, A in this article's Online Repository at [www.jacionline.org](http://www.jacionline.org)). In keeping with these observations, murine DCs from Ttc7-deficient mice also present with an increased cell death on chemotactic migration in collagen gels (Fig E6, B). This suggests that increased mortality of TTC7A-deficient cells in the presence of CCL21 was a consequence of cell confinement and correlated with the capacity of CCL21 to form long haptotactic gradients by binding to collagen fibers. Then, we sought to evaluate whether the increased mortality of TTC7A-deficient cells was related to DNA damage in this microenvironment. To do so, 53BP1 foci

staining on nucleus was used as indicator of DNA damage. We found low levels of DNA damage in absence of confinement in both cell types (Fig E6, C). An increased DNA damage was observed in chemotactic conditions in TTC7A-deficient T-cell blasts (Fig 6, D and E). Supplementing TTC7A-deficient T cells and murine DC<sup>fsm</sup> with PI4P protected cells from DNA damage and death during directional migration in collagen gels (Fig 6, B and C and Fig E6, B). Alternatively, inhibition of PI4KIII $\alpha$  or AKT activity in control T-cell blasts, recapitulated the increased cell death and DNA damage observed in TTC7A-deficient cells (Fig E6, D-F). In keeping with these data, freshly isolated PBMCs from TTC7A-deficient patients presented increased DNA damage compared to control cells (Fig 6, F). These results indicate that alterations in actin dynamics caused by defective PI4KIII $\alpha$ /PI3K/AKT/RHOA signaling in TTC7A-deficient cells are associated with an impaired nuclear deformation, resulting in increased DNA damage and reduced survival in response to chemotactic signals in complex 3D microenvironments.

Thus, TTC7A acts as a critical regulator of human T-cell migration and cell survival under confinement, suggesting that

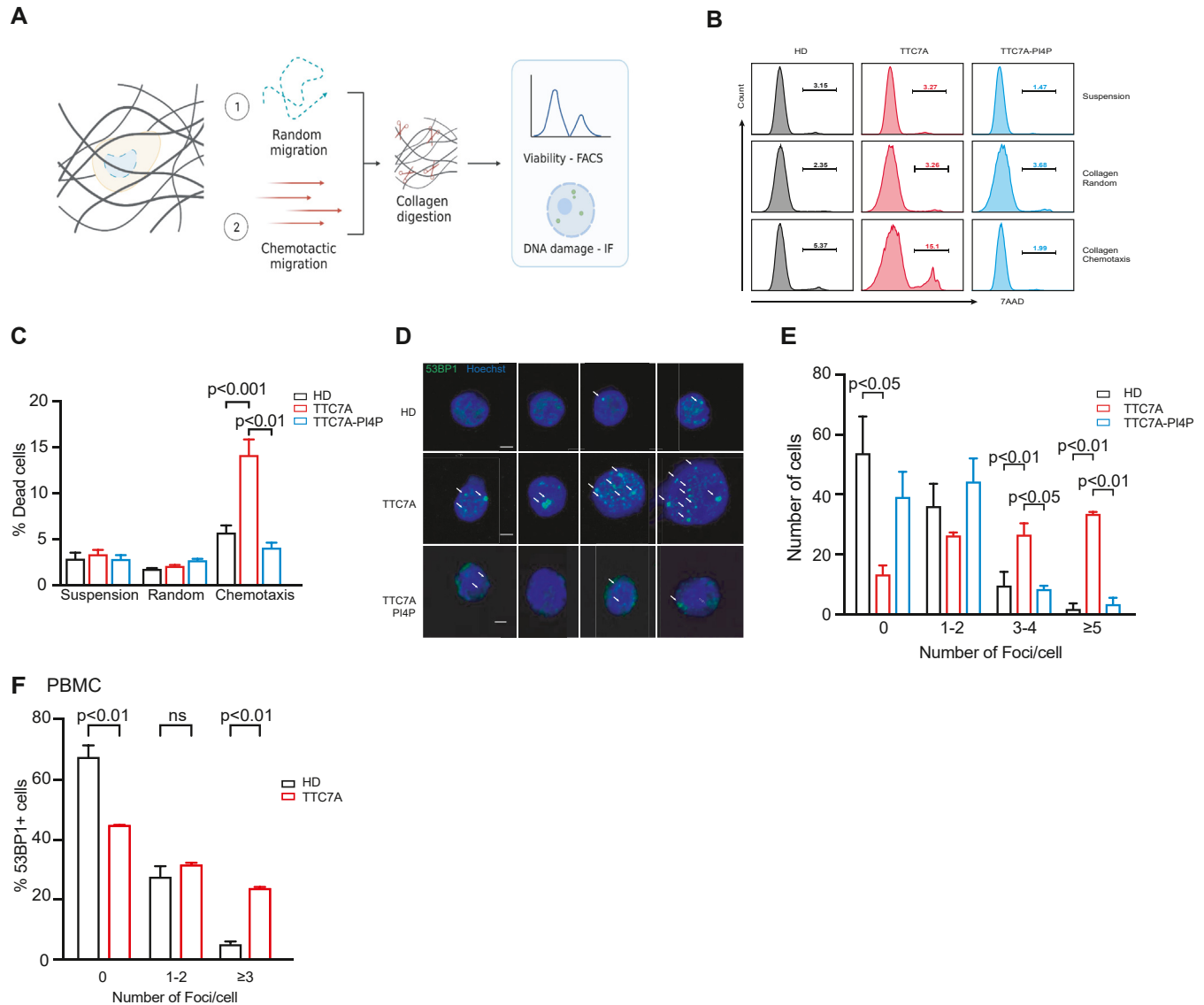


**FIG 6.** TTC7A is required for T-cell blast survival when migrating in dense microenvironments. **(A)** Experimental design, T-cell blasts were embedded into highly dense collagen and allowed to migrate randomly or in response to CCL21 for 48 hours; collagen was digested with collagenase; DNA damage and viability were evaluated in recovered cells. **(B)** Representative histograms depicting 7-aminoactinomycin D (7AAD)-positive cells in suspension, random collagen, and chemotactic collagen for HD (black), TTC7A (red), and TTC7A-PI4P (blue) T-cell blast. **(C)** Percentage of dead cells for HD (black empty bars), TTC7A (red empty bars), and TTC7A-PI4P (blue empty bars) T cells ( $n = 8$ ). Bars represent mean and error bars the SEM. **(D)** 53BP1 staining of HD, TTC7A, and TTC7A-PI4P T cells recovered from collagens. Bar = 3  $\mu\text{m}$ . **(E)** Quantification of the number of 53BP1 foci per cell for HD, TTC7A, and TTC7A-PI4P T cells ( $n > 130$  cells/condition). Bars represent mean and error bars the SEM. **(F)** Quantification of the number of 53BP1 foci per cell in PBMCs from HD (black empty bars) and TTC7A-deficient (red empty bars) cells ( $n = 3$ ). Two-way ANOVA was applied for statistical analysis in **C**, **E**, and **F**. NS, Not significant.

alterations of this process may contribute to dysregulated immune homeostasis observed in TTC7A-deficient patients.

## DISCUSSION

TTC7A participates in several cellular functions.<sup>2,10,11,24,25</sup> However, it is not clear how alterations in these processes contribute to the immune phenotype characterizing TTC7A-deficient patients. This report shows that TTC7A is a regulator

of leukocyte migration in humans and mice. TTC7A controls F-actin polymerization at the different poles of the cell by ensuring the activity of the PI4KIII $\alpha$ /PI3K/AKT/RHOA regulatory axis. The synthesis of PI4P is the first step of a signaling pathway leading to PI(3,4,5)P<sub>3</sub> production, AKT activation, and eventually RHOA activity,<sup>20</sup> among many others.<sup>26</sup> TTC7A deficiency decreases kinase activity of PI4KIII $\alpha$ , reducing the pool of PI4P,<sup>8,27</sup> leading to RHOA hyperactivation. Subsequently, RHOA destabilizes the autoinhibited conformation of the DIAPH1,

promoting the polymerization of actin filaments and persistent motility.<sup>28,29</sup> In murine DCs, the coordinated action of mDia1 and Arp2/3 controls migration by promoting actin polymerization at the front or back of the cell.<sup>15</sup> Our results support that similar mechanisms occur in human lymphocytes. The increase DIAPH1 activity observed in TTC7A-deficient cells suggests that a competition between DIAPH1 and ARP2/3 for free actin monomers could modulate their activities and thus actin dynamics and cell migration. Such a regulatory loop has been described in yeasts, amoebas, drosophila, and mammalian cells, because depletion or inhibition of one actin regulator increases the activity of the other.<sup>30,31</sup>

Surprisingly, it was found that TTC7A-deficient T-cell blasts present different phenotypes depending on the complexity of the surrounding microenvironment. In microchannels, which allowed us to assess the intrinsic contractility of cells in an obstacle-free microenvironment, TTC7A-deficient cells have increased speed as compared to controls, independent of the coating (ie, fibronectin or collagen). On the contrary, TTC7A-deficient cells were slower in collagen gels (ie, 3D environment), which impose cell deformations during migration. This dichotomy can be explained by the fact that despite having stronger contractility, TTC7A-deficient cells have an impaired capacity to deform and pass through micrometric constrictions. This suggests that cell and nuclear deformations are the limiting factors determining migration capacity in tissues.<sup>32,33</sup>

During interstitial migration, leukocytes deform their nucleus in an ARP2/3-dependent process.<sup>22,34</sup> As a consequence of this deformation, the nucleus suffers a high degree of mechanical stress, which can be associated with ruptures of the nuclear envelope and DNA exposure to the cytoplasm.<sup>35-37</sup> In control cells, migration-induced DNA damage is prevented by the fast resealing of the nuclear envelope.<sup>36</sup> In context of TTC7A deficiency, alterations in front-back actin polymerization reduce their deformation capacity leading to accumulation of DNA damage and reduced cell survival during chemotactic response in complex microenvironments. Our results suggest that alterations in leukocyte migration could constitute a pathophysiological mechanism underlying the progressive lymphopenia reported in TTC7A-deficient patients.

Our work raises intriguing questions as to whether alterations in leukocyte migration contribute to immunodeficiency in other primary immunodeficiency diseases. It has been shown that mutations in DOCK8 lead to leukocyte susceptibility to undergo a form of cell death known as cytothripsis,<sup>38</sup> which has been proposed to be caused by the loss of front/rear coordination during displacement.<sup>38</sup> In contrast to what has been reported for DOCK8, cytothripsis was not observed in TTC7A-deficient leukocytes, suggesting that TTC7A is not required to preserve cell shape during motility. Leukocyte migration could also be defective in other primary immunodeficiency diseases associated with defects in the production of PI4P (or other metabolites of this pathway), as is the case for the recently described mutations in *PI4KA*<sup>39,40</sup> in patients with a clinical phenotype partially resembling patients with multiple intestinal atresia—combined immunodeficiency.<sup>1,41</sup> (ie, caused by *TTC7A* null mutations). Based on our data, lymphocytes from patients who are *PI4KA*-deficient will likely display similar motility defects. Alterations in leukocyte migration could also contribute to pathophysiology in other conditions such as defects of DNA damage response machinery.<sup>42,43</sup> Indeed, ATR and ATM are required for repair of DNA

damage and preservation of DNA integrity during migration under confinement.<sup>35,36</sup> However, it is not known whether alterations in this process contribute to clinical phenotypes.

In conclusion, we unveil TTC7A as a critical regulator of actin dynamics, allowing lymphocytes to efficiently migrate in complex microenvironments. Our data suggest that alterations in cell motility can lead to accumulation of DNA damage and reduce cell viability. Therefore, we propose that alterations in nuclear mechanics in lymphocytes during confined migration could play a previously unappreciated pathophysiological role in the development of progressive lymphopenia and immunodeficiency.

## DISCLOSURE STATEMENT

This work was supported by the state funding from the Agence Nationale de la Recherche under “Investissements d’avenir” program (ANR-10-IAHU-01), and the French National Institute of Health and Medical Research (INSERM). T.G. was supported by the International PhD program of the Imagine Institute and the Fondation Bettencourt Schueller. M.B. was supported by Emergence Cancerpole Ile-de-France (Syntec), ATEurope, and Institut Pierre-Gilles de Gennes High Risk/High Gain. M.L. was supported by the Imagine Institute (WP05T012). F.E.S. received funding and supports from The Agence Nationale de la Recherche (ANR-18-CE15-0017), the ARC Foundation (PJA 20191209614), La Ligue Contre le Cancer (RS19/75-79, RS20/75-30). G.M. received funding and support from La Ligue Contre le Cancer (RS21/75-3) and the ARC foundation (PJA 20181207755). P.V. received funding and support from the Agence Nationale de la Recherche (ANR-16-CE13-0009, ANR-21-CE17-0050, ANR-20-CE15-0019, Labex-IPGG ANR-10-IDEX-0001-02 PSL and ANR-10-LABX-31).

Disclosure of potential conflict of interest: The authors declare that they have no relevant conflicts of interest.

The authors thank the Imagerie Cellulaire and the Bio-Image Analysis platforms of the SFR Necker for their technical support with live microscopy experiments and image analysis. We thank Matthieu Bernard for precious help to accelerate image processing, Manon Brouard for help with Epoxy molds, and P. J. Saéz for initial help. We are grateful to Marta Mastrogianni for sharing her expertise on T cells. Fig 6, A and the graphical abstract were created with [biorender.com](https://biorender.com)

**Clinical implications: TTC7A controls actin dynamics, leukocyte motility and survival in 3D environments. Our data offer a likely explanation for the progressive lymphopenia observed in patients and highlight alterations in cell motility as a putative pathophysiological mechanism.**

## REFERENCES

1. Bigorgne AE, Farin HF, Lemoine R, Mahlaoui N, Lambert N, Gil M, et al. TTC7A mutations disrupt intestinal epithelial apical-basal polarity. *J Clin Invest* 2014;124:328-37.
2. Lemoine R, Pachlopnik-Schmid J, Farin HF, Bigorgne A, Debre M, Sepulveda F, et al. Immune deficiency-related enteropathy-lymphocytopenia-alopecia syndrome results from tetratricopeptide repeat domain 7A deficiency. *J Allergy Clin Immunol* 2014;134:1354-1364e6.
3. Avitzur Y, Guo C, Mastroaolo LA, Bahrami E, Chen H, Zhao Z, et al. Mutations in tetratricopeptide repeat domain 7A result in a severe form of very early onset inflammatory bowel disease. *Gastroenterology* 2014;146:1028-39.
4. El-Daher MT, Lemale J, Bruneau J, Leveau C, Guerin F, Lambert N, et al. Chronic intestinal pseudo-obstruction and lymphoproliferative syndrome as a novel



- phenotype associated with tetratricopeptide repeat domain 7A deficiency. *Front Immunol* 2019;10:2592.
5. Lien R, Lin YF, Lai MW, Weng HY, Wu RC, Jaing TH, et al. Novel mutations of the tetratricopeptide repeat domain 7A gene and phenotype/genotype comparison. *Front Immunol* 2017;8:1066.
  6. Lees JA, Zhang Y, Oh MS, Schauder CM, Yu X, Baskin JM, et al. Architecture of the human PI4KIIIalpha lipid kinase complex. *Proc Natl Acad Sci U S A* 2017; 114:13720-5.
  7. Chung J, Nakatsu F, Baskin JM, De Camilli P. Plasticity of PI4KIIIalpha interactions at the plasma membrane. *EMBO Rep* 2015;16:312-20.
  8. Nakatsu F, Baskin JM, Chung J, Tanner LB, Shui G, Lee SY, et al. PtdIns4P synthesis by PI4KIIIalpha at the plasma membrane and its impact on plasma membrane identity. *J Cell Biol* 2012;199:1003-16.
  9. Batrouni AG, Baskin JM. The chemistry and biology of phosphatidylinositol 4-phosphate at the plasma membrane. *Bioorg Med Chem* 2021;40:116190.
  10. El-Daher MT, Cagnard N, Gil M, Da Cruz MC, Leveau C, Sepulveda F, et al. Tetratricopeptide repeat domain 7A is a nuclear factor that modulates transcription and chromatin structure. *Cell Discov* 2018;4:61.
  11. Leveau C, Gajardo T, El-Daher MT, Cagnard N, Fischer A, de Saint Basile G, et al. Ttc7a regulates hematopoietic stem cell functions while controlling the stress-induced response. *Haematologica* 2020;105:59-70.
  12. Vargas P, Terriac E, Lennon-Dumenil AM, Piel M. Study of cell migration in microfabricated channels. *J Vis Exp* 2014;84:e51099.
  13. Jacobelli J, Friedman RS, Conti MA, Lennon-Dumenil AM, Piel M, Sorensen CM, et al. Confinement-optimized three-dimensional T cell amoeboid motility is modulated via myosin IIA-regulated adhesions. *Nat Immunol* 2010;11:953-61.
  14. Heuze ML, Vargas P, Chabaud M, Le Berre M, Liu YJ, Collin O, et al. Migration of dendritic cells: physical principles, molecular mechanisms, and functional implications. *Immunol Rev* 2013;256:240-54.
  15. Vargas P, Maiuri P, Bretou M, Saez PJ, Pierobon P, Maurin M, et al. Innate control of actin nucleation determines two distinct migration behaviours in dendritic cells. *Nat Cell Biol* 2016;18:43-53.
  16. Bretou M, Saez PJ, Sanseau D, Maurin M, Lankar D, Chabaud M, et al. Lysosome signaling controls the migration of dendritic cells. *Sci Immunol* 2017;2:eaak9573.
  17. Bros M, Haas K, Moll L, Grabbe S. RhoA as a key regulator of innate and adaptive immunity. *Cells* 2019;8:733.
  18. Dornan GL, Dalwadi U, Hamelin DJ, Hoffmann RM, Yip CK, Burke JE. Probing the architecture, dynamics, and inhibition of the PI4KIIIalpha/TTC7/FAM126 complex. *J Mol Biol* 2018;430:3129-42.
  19. Baird D, Stefan C, Audhya A, Weys S, Emr SD. Assembly of the PtdIns 4-kinase Stt4 complex at the plasma membrane requires Ypp1 and Efr3. *J Cell Biol* 2008; 183:1061-74.
  20. Papakonstanti EA, Ridley AJ, Vanhaesebroeck B. The p110delta isoform of PI 3-kinase negatively controls RhoA and PTEN. *EMBO J* 2007;26:3050-61.
  21. Vargas P, Barbier L, Saez PJ, Piel M. Mechanisms for fast cell migration in complex environments. *Curr Opin Cell Biol* 2017;48:72-8.
  22. Thiam HR, Vargas P, Carpi N, Crespo CL, Raab M, Terriac E, et al. Perinuclear Arp2/3-driven actin polymerization enables nuclear deformation to facilitate cell migration through complex environments. *Nat Commun* 2016;7:10997.
  23. Nader GPF, Aguera-Gonzalez S, Routet F, Gratia M, Maurin M, Cancila V, et al. Compromised nuclear envelope integrity drives TREX1-dependent DNA damage and tumor cell invasion. *Cell* 2021;184:5230-46.e22.
  24. Jardine S, Anderson S, Babcock S, Leung G, Pan J, Dhingani N, et al. Drug screen identifies leflunomide for treatment of inflammatory bowel disease caused by TTC7A deficiency. *Gastroenterology* 2020;158:1000-15.
  25. Jardine S, Dhingani N, Muise AM. TTC7A: steward of intestinal health. *Cell Mol Gastroenterol Hepatol* 2019;7:555-70.
  26. Tzenaki N, Papakonstanti EA. p110delta PI3 kinase pathway: emerging roles in cancer. *Front Oncol* 2013;3:40.
  27. Baskin JM, Wu X, Christiano R, Oh MS, Schauder CM, Gazzero E, et al. The leukodystrophy protein FAM126A (hycin) regulates PtdIns(4)P synthesis at the plasma membrane. *Nat Cell Biol* 2016;18:132-8.
  28. Vicente-Manzanares M, Rey M, Perez-Martinez M, Yanez-Mo M, Sancho D, Cabrero JR, et al. The RhoA effector mDia is induced during T cell activation and regulates actin polymerization and cell migration in T lymphocytes. *J Immunol* 2003; 171:1023-34.
  29. Kuhn S, Geyer M. Formins as effector proteins of Rho GTPases. *Small GTPases* 2014;5:e29513.
  30. Davidson AJ, Wood W. Unravelling the actin cytoskeleton: a new competitive edge? *Trends Cell Biol* 2016;26:569-76.
  31. Buracco S, Claydon S, Insall R. Control of actin dynamics during cell motility. *F1000Res* 2019;8:F1000 Faculty Rev-1977.
  32. Huse M. Mechanical forces in the immune system. *Nat Rev Immunol* 2017;17: 679-90.
  33. Lammermann T, Bader BL, Monkley SJ, Words T, Wedlich-Soldner R, Hirsch K, et al. Rapid leukocyte migration by integrin-independent flowing and squeezing. *Nature* 2008;453:51-5.
  34. Calero-Cuenca FJ, Janota CS, Gomes ER. Dealing with the nucleus during cell migration. *Curr Opin Cell Biol* 2018;50:35-41.
  35. Kidiyoor GR, Li Q, Bastianello G, Bruhn C, Giovannetti I, Mohamood A, et al. ATR is essential for preservation of cell mechanics and nuclear integrity during interstitial migration. *Nat Commun* 2020;11:4828.
  36. Raab M, Gentili M, de Belly H, Thiam HR, Vargas P, Jimenez AJ, et al. ESCRT III repairs nuclear envelope ruptures during cell migration to limit DNA damage and cell death. *Science* 2016;352:359-62.
  37. Nader GPF, Williard A, Piel M. Nuclear deformations, from signaling to perturbation and damage. *Curr Opin Cell Biol* 2021;72:137-45.
  38. Zhang Q, Dove CG, Hor JL, Murdock HM, Strauss-Albee DM, Garcia JA, et al. DOCK8 regulates lymphocyte shape integrity for skin antiviral immunity. *J Exp Med* 2014;211:2549-66.
  39. Salter CG, Cai Y, Lo B, Helman G, Taylor H, McCartney A, et al. Biallelic PI4KA variants cause neurological, intestinal and immunological disease. *Brain* 2021;144: 3597-610.
  40. Verdura E, Rodriguez-Palmero A, Velez-Santamaria V, Planas-Serra L, de la Calle I, Raspall-Chaure M, et al. Biallelic PI4KA variants cause a novel neurodevelopmental syndrome with hypomyelinating leukodystrophy. *Brain* 2021;144: 2659-69.
  41. Wu X, Chi RJ, Baskin JM, Lucast L, Burd CG, De Camilli P, et al. Structural insights into assembly and regulation of the plasma membrane phosphatidylinositol 4-kinase complex. *Dev Cell* 2014;28:19-29.
  42. Gennery AR. Primary immunodeficiency syndromes associated with defective DNA double-strand break repair. *Br Med Bull* 2006;77-78:71-85.
  43. Tiwari V, Wilson DM 3rd. DNA damage and associated DNA repair defects in disease and premature aging. *Am J Hum Genet* 2019;105:237-57.